American Mineralogist, Volume 74, pages 896–901, 1989

Coupled substitutions involving REEs and Na and Si in apatites in alkaline rocks from the Ilímaussaq intrusion, South Greenland, and the petrological implications*

Jørn G. Rønsbo
Institut for Mineralogi, Københavns Universitet, Øster Voldgade 10, DK-1350 Copenhagen, Denmark

Abstract

Apatites from the Ilímaussaq augite syenite, the sodalite foyaite, and a quartz-bearing peralkaline pegmatite have been analyzed using an electron microprobe for the major elements plus Na, Si, and selected rare-earth elements (REEs). In all three rock types, the maximum REE_2O_3 content in the apatite exceeds 16.0 wt%. Apatite from the augite syenite and primary apatite from the sodalite foyaite are characterized by a low Na content that varies independently of the REE content. The composition of these apatites approaches 25 mol% of the end-member $Ca_2REE_3(SiO_4)_3(OH,F,Cl)$ (lessingite) in response to the substitution $REE^{3+} + Si^{4+} \rightleftharpoons Ca^{2+} + P^{5+}$. REE- and Na-enriched apatites from the quartz-bearing peralkaline pegmatite are almost Si free, and REEs and Na are positively correlated. The composition of these apatites approaches 25 mol% of the hypothetical end-member $Na_5REE_5(PO_4)_6(OH,F,Cl)_2$, in response to the substitution $Na^+ + REE^{3+} \rightleftharpoons 2Ca^{2+}$. The compositional trend of late-crystallizing apatite from the sodalite foyaite reflects almost equal contributions of the two substitutions. The relationship between these substitutions in a given apatite and its associated mineral assemblage indicates that the Na component is only present in considerable amounts when apatite crystallizes in a strongly peralkaline environment.

Introduction

In many crustal rocks, apatite is of major geochemical importance, being one of the minerals in which the rare-earth elements (La to Lu + Y = REEs) concentrate. However, in most rocks, even the more evolved, the REE content in apatite is low and does not reflect possible maximum enrichment as outlined in the experimental investigations by Ito (1968) and Watson and Green (1981). Unusually REE-rich apatites are found in nepheline syenites from the Ilímaussaq intrusion and related phonolitic dykes, as indicated by Larsen (1979) and briefly outlined by Rønsbo (1986).

This paper describes the chemical variation in REE-enriched apatite from the Ilímaussaq intrusion with the objectives of substantiating two different types of substitutions that result in REE enrichment and demonstrating their dependence on magma alkalinity.

Geologic setting and sample description

The Ilímaussaq intrusion belongs to the late Precambrian magmatic Gardar Province of South Greenland, which consists of numerous volcanic and plutonic alkaline rocks (Upton, 1974; Emeleus and Upton, 1976). The most undersaturated and differentiated alkaline rocks occur in the Ilímaussaq intrusion, which is characterized by an unusual enrichment in incompatible elements such as Zr, Nb, La, Ce, U, and Th. Three major intrusive events can be outlined on the basis of field relationships (Steenfelt, 1981) plus mineralogical and geochemical data (Blaxland et al., 1976; Larsen, 1976; Sørensen, 1978). These are represented by an augite syenite shell, alkaline granitic sheets in the top of the intrusion, and the volumetrically dominant sequence of layered agpaitic nepheline syenites in the central part of the intrusion (Fig. 1). The samples examined in the present study are from the innermost part of the augite syenite, the roof sequence of layered agpaitic nepheline syenites, and a peralkaline quartz-bearing pegmatite from outside the intrusion.

Augite syenite

The augite syenite magma was the first to be emplaced, and the augite syenite shell along the sides and roof of the intrusion has a chilled margin toward the country rocks. The augite syenite is supposed to be mainly cumulous (Bailey et al., 1981) with Fe-rich olivine, ferrosalite, ternary feldspar, apatite, and titanomagnetite as the liquidus phases. The slightly silica-undersaturated magma was not peralkaline, but crystal fractionation produced a residual liquid of nepheline syenite composition. For the present study, a sample from the innermost facies with interstitial nepheline was chosen (GGU no. 150722, also used by Larsen, 1976).

Nepheline syenites

The third and major pulse of magma was peralkaline and silica undersaturated and led to the formation of a

* Contribution to the mineralogy of Ilímaussaq no. 84.

0003–004X/89/0708–0896$02.00

TABLE 1. REEs (wt%) in Durango apatite

	This paper	Young et al. (1969)	Rogers et al. (1984)	Roeder et al. (1987)
La_2O_3	0.474 (0.015)	0.493	0.416	0.414
Ce_2O_3	0.563 (0.022)	0.550	0.517	0.505
Pr_2O_3	0.040 (0.007)	<0.117	0.050	0.069
Nd_2O_3	0.148 (0.007)	0.233	0.150	0.151
Sm_2O_3	0.024 (0.007)	0.035	<0.006	0.019
Dy_2O_3	0.017 (0.006)	0.017	0.026	0.021
Yb_2O_3	0.007 (0.007)	0.006	0.011	0.006
Y_2O_3	0.093 (0.005)	0.097	n.d.	0.072

Note: This paper, electron-microprobe analysis. Young et al. (1969); DM-A, optical spectography (analyst N. M. Conklin). Rogers et al. (1984), proton-induced X-ray emission. Roeder et al. (1987), proton-induced X-ray emission. Standard deviations in parentheses.

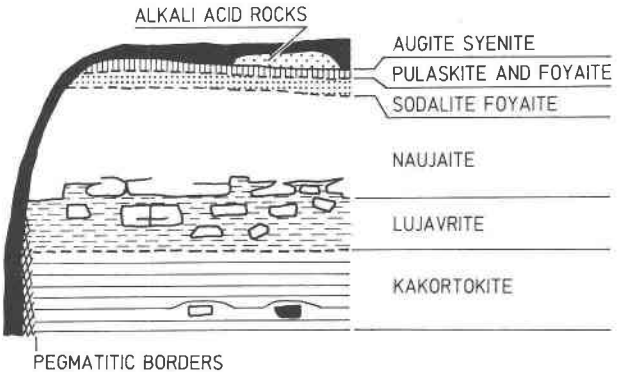

Fig. 1. Diagrammatic E-W cross section of the southern part of the Ilímaussaq intrusion (modified after Andersen et al., 1981).

layered series of cumulus miaskitic and agpaitic nepheline syenites in which a roof sequence (pulaskite, foyaite, sodalite foyaite, and naujaite), a floor sequence (kakortokite), and a "sandwich" sequence (lujavrite) can be discerned (Fig. 1).

The roof sequence is generally thought to have formed by successive downward crystallization from a single magma (Ferguson, 1964; Larsen, 1976; Larsen and Sørensen, 1987) that became more and more differentiated and volatile rich. During the early stage of crystallization, the anhydrous high-temperature liquidus mineral assemblage included alkali feldspar, hedenbergite, fayalite, titanomagnetite, and apatite (Larsen, 1976). These minerals constitute the major part of the pulaskite and foyaite. Sodalite and nepheline were added to the liquidus mineral assemblage in the sodalite foyaite and naujaite (Larsen, 1976). During the formation of the roof sequence, hedenbergite, fayalite, and titanomagnetite reacted and were replaced by alkali amphibole, aegirine, and aenigmatite. These phases are the dominant Fe-bearing silicates in the sodalite foyaite and naujaite, where the mafic high-temperature liquidus minerals only occur in minor amounts (<1 vol%, Larsen, 1976). A sodalite foyaite sample (GGU no. 149532) with an exceptionally high content of the anhydrous high-temperature liquidus mineral assemblage was chosen for study. This sample was also analyzed by Larsen (1976).

Quartz-bearing peralkaline pegmatite

The sample examined (GGU no. 177244) is from one of two pegmatite veins, approximately 20 m long and up to 10 cm thick, in a fine-grained granite close to the contact between the Ilímaussaq intrusion and the basement in the Kangerdluarssuk fjord area (H. Bohse, personal communication). Both veins are surrounded by distinct fenitization zones. The vein from which sample GGU no. 177244 was taken has a 5-mm-thick melanocratic border zone dominated by aegirine, and a central zone containing up to 2-cm-long aegirine crystals. The central zone is dominated by fine-grained euhedral albite and subordinate amounts of K-feldspar, apatite, aegirine, and thorite, which are poikilitically enclosed in anhedral eudialyte and quartz. In some parts of the vein, arfvedsonite occurs as interstitial grains and as a replacement of aegirine. The veins are inferred to be hybrids formed of partly mobilized basement granite and a peralkaline liquid (H. Bohse, personal communication).

Analytical methods, apatite occurrence, and apatite chemistry

Analytical methods

The apatites were analyzed on a JEOL 733 Superprobe using the JEOL software PACX-M for instrumental control and ZAF correction. The analyses were performed at 15 kV, and with a beam current of 15–60 nA. The following spectral lines and standards were used: P$K\alpha$, Ca$K\alpha$, F$K\alpha$, Wilbuforce apatite; Si$K\alpha$, wollastonite; Na$K\alpha$, jadeite; Ce$L\alpha$, CeO_2; La$L\alpha$, silicate glass containing 18.0 wt% La_2O_3; Pr$L\beta$, $Pr_3Ga_5O_{12}$; Nd$L\alpha$, $Nd_3Ga_5O_{12}$; Sm$L\alpha$, $SmFeO_3$; Dy$L\alpha$ and Yb$L\alpha$, synthetic glass standards (Drake and Weill, 1972); Y$L\alpha$, $Y_3Al_5O_{12}$. The net peak intensities were corrected for peak-peak overlap, as well as peak interference on background positions. Durango apatite (Young et al., 1969) and a number of synthetic glass standards prepared by Drake and Weill (1972) have been analyzed many times during a one-year period, and the reproducibility of the results listed in Tables 1 and 2 is very good. The synthetic glass standards prepared by Roeder (1985) have been analyzed only once, collecting counts for 10 s on each of 60 points. For that reason, only results for the low-REE-concentration glass (no. S-253)

TABLE 2. REEs (wt%) in Drake and Weill glasses

	This paper	Drake and Weill (1972) a	Drake and Weill (1972) b	Roeder (1985)
La_2O_3	4.39 (0.05)	4.28	4.59	4.22
Ce_2O_3	3.96 (0.11)	4.00	4.30	3.84
Pr_2O_3	4.18 (0.07)	4.44	4.60	4.28
Nd_2O_3	4.11 (0.13)	4.26	4.20	4.26
Sm_2O_3	4.44 (0.05)	4.26	4.31	4.38

Note: This paper, electron-microprobe analysis. Drake and Weill (1972); a, nominal wt% from initial weighing; b, neutron activation analysis. Roeder (1985), electron-microprobe analysis. Standard deviations in parentheses.

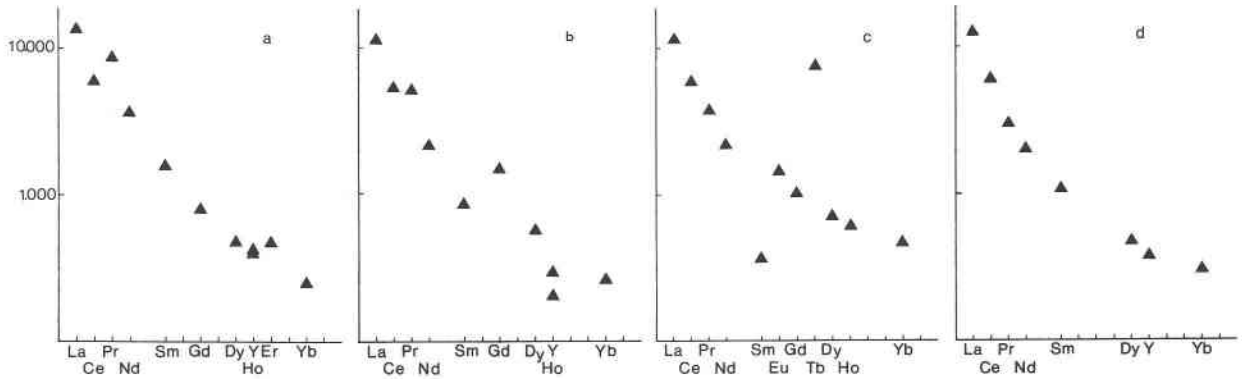

Fig. 2. Chondrite-normalized REEs of the Durango apatite: (**a**) Young et al. (1969); (**b**) Roeder et al. (1987); (**c**) Rogers et al. (1984); (**d**) this study.

are given (Table 3). The electron-microprobe analyses of the glass standards are in good agreement with the published results for most elements using other analytical methods (Tables 2 and 3).

The electron-microprobe analysis of the Durango apatite is compared with analyses of different samples from the same locality (Table 1). The present results for La_2O_3 and Ce_2O_3 agree well with the spectrographic analysis of Young et al. (1969), but differ from the analysis of Rogers et al. (1984) and Roeder et al. (1987). The differing results may indicate natural heterogeneity. For this reason, an evaluation of the REE analyses of the Durango apatite presented in this paper can most reasonably be done using the chondrite-normalized REE spectrum, assuming that despite different concentration levels, the normalized concentration profiles will have the same shape. The chondrite-normalized spectra are plotted in Figures 2a–2d. Except for Pr (Fig. 2a, Young et al., 1969) and Sm and Tb (Fig. 2c, Rogers et al., 1984), the chondrite-normalized profiles have the same shape; the microprobe results presented in this paper show the least scatter. The analyses of synthetic glasses and Durango apatite show that the electron-microprobe method applied in this investigation is very reliable, even for low REE concentrations.

TABLE 3. REEs (wt%) in glass S-253 (Roeder 1985)

	This paper	Roeder (1985)	Roeder et al. (1987) a	b	c
La	0.08 (0.01)	0.08	0.073	0.088	0.06
Ce	0.08 (0.01)	0.08	0.072	0.083	0.06
Pr	0.08 (0.02)	0.08	0.076	—	0.08
Nd	0.08 (0.01)	0.08	0.076	0.083	0.08
Sm	0.08 (0.02)	0.08	0.068	0.086	0.06
Dy	0.07 (0.02)	0.08	0.095	0.080	0.06
Yb	0.07 (0.03)	0.08	0.076	0.081	0.06
Y	0.08 (0.01)	0.08			

Note: This paper, electron-microprobe analysis. Roeder (1985), nominal wt% from initial weighing. Roeder et al. (1987); a, proton-induced X-ray emission analysis; b, neutron activation analysis (average of three different analyses); c, electron-microprobe analysis. Standard deviation in parentheses.

Apatite occurrence and chemistry

Augite syenite. Samples from the chilled margin and the middle part are rich in 0.05- to 0.3-mm apatite, which occurs as inclusions in the other liquidus phases. In a sample from the innermost facies, only two apatite crystals have been observed. One is a 1.0 × 0.5 mm euhedral crystal, whereas the other is an interstitial, irregular grain. The major part of the euhedral crystal is homogeneous (based on a back-scattered electron image) with a total REE content of approximately 1 wt% REE_2O_3 (Table 4,

TABLE 4. Microprobe analyses of Na-poor, REE-enriched apatite

	Augite syenite GGU 150722			Sodalite foyaite GGU 149532	
	1	2	3	4	5
P_2O_5	41.11	37.85	28.16	29.62	26.66
SiO_2	0.39	2.16	7.32	6.67	8.17
CaO	55.00	51.54	41.45	43.64	40.40
Na_2O	0.05	0.06	0.00	0.15	0.15
La_2O_3	0.18	1.19	3.67	3.17	4.07
Ce_2O_3	0.43	2.71	7.89	7.27	8.90
Pr_2O_3	0.06	0.30	0.89	0.82	1.01
Nd_2O_3	0.23	1.37	3.46	3.48	4.14
Sm_2O_3	0.05	0.32	0.67	0.61	0.76
Dy_2O_3	0.03	0.20	0.29	n.a.	n.a.
Y_2O_3	0.10	0.50	1.75	1.03	1.14
F	3.65	4.10	2.20	4.30	4.43
Cl	<0.01	0.02	0.04	0.04	0.01
	101.29	102.32	97.79	100.80	99.84
F,Cl ≡ −O	1.55	1.76	0.96	1.82	1.87
Total	99.74	100.56	96.83	98.98	97.83
	Cations based on 25 oxygens				
P	5.90	5.59	4.61	4.74	4.43
Si	0.07	0.38	1.42	1.26	1.60
Ca	10.00	9.63	8.59	8.84	8.49
Na	0.02	0.02	0.00	0.06	0.06
La	0.01	0.08	0.26	0.22	0.30
Ce	0.03	0.17	0.56	0.51	0.64
Pr	0.00	0.02	0.06	0.06	0.07
Nd	0.01	0.09	0.24	0.24	0.28
Sm	0.00	0.02	0.04	0.04	0.05
Dy	0.00	0.01	0.02	n.a.	n.a.
Y	0.01	0.05	0.18	0.10	0.12

Note: Augite syenite: 1, central part of euhedral crystal; 2, slightly REE-enriched part of overgrowth on interstitial crystal; 3, rim zone of crystal 2. Sodalite foyaite: 4 and 5, oscillatory-zoned primary apatite.

TABLE 5. Microprobe analyses of Na-bearing, REE-enriched apatite

	Sodalite foyaite GGU 149532				Peralkaline pegmatite GGU 177244		
	1	2	3	4	5	6	7
P_2O_5	39.20	38.20	36.43	36.11	40.37	38.53	37.50
SiO_2	1.21	1.55	2.05	2.49	0.17	0.32	0.39
CaO	50.20	48.84	46.99	43.97	52.64	46.14	38.30
Na_2O	0.68	0.77	1.09	1.63	0.61	1.95	3.09
La_2O_3	2.05	2.41	3.57	3.27	0.49	3.27	4.95
Ce_2O_3	2.95	3.80	5.03	6.47	1.43	5.16	8.79
Pr_2O_3	0.33	0.45	0.51	0.60	0.20	0.79	0.70
Nd_2O_3	0.99	1.13	1.50	2.30	0.85	1.28	2.23
Sm_2O_3	0.15	0.17	0.19	0.66	n.a.	n.a.	n.a.
Y_2O_3	0.10	0.17	0.26	0.46	n.a.	n.a.	n.a.
F	4.60	4.28	n.a.	3.07	n.a.	n.a.	n.a.
Cl	0.01	0.02	n.a.	0.02	n.a.	n.a.	n.a.
	102.47	101.79	97.62	101.05	96.76	97.44	95.95
F,Cl ≡ −O	1.94	1.80		1.29			
Total	100.53	99.99		99.76			
Cations based on 25 oxygens							
P	5.78	5.71	5.56	5.56	5.92	5.86	5.95
Si	0.21	0.27	0.37	0.45	0.03	0.06	0.07
Ca	9.37	9.24	9.07	8.57	9.77	8.87	7.69
Na	0.23	0.26	0.38	0.58	0.20	0.68	1.12
La	0.13	0.16	0.24	0.22	0.03	0.22	0.34
Ce	0.19	0.25	0.33	0.43	0.09	0.34	0.69
Pr	0.02	0.03	0.03	0.04	0.00	0.05	0.05
Nd	0.06	0.07	0.10	0.15	0.05	0.08	0.15
Sm	0.01	0.01	0.01	0.04	n.a.	n.a.	n.a.
Y	0.01	0.02	0.02	n.a.	n.a.	n.a.	n.a.

Note: Sodalite foyaite: 1 and 2, oscillatory-zoned part of late magmatic euhedral crystal; 3, irregularly zoned central part of crystal 1 and 2; 4, overgrowth on irregularly zoned crystal. Peralkaline pegmatite: 5 and 7, irregularly zoned rim on euhedral crystal; 6, oscillatory-zoned core of crystal in analyses 5 and 7.

analysis 1). The outermost 50–100 μm of the crystal displays a distinct REE enrichment. Comparable REE enrichment is found in the intercumulus apatite overgrowth on the irregular grains (Table 4, analyses 2 and 3). Here the highest recorded total REE_2O_3 content is approximately 18 wt%. In all analyses, Ce is the dominant REE. La and Nd are present in almost equal amounts, but increasing La/Nd ratios (0.78, 0.86, and 1.06) indicate a relative La enrichment with increasing REE content. Inspection of the analyses in Table 4 shows that the increasing REE contents are accompanied by increasing Si contents, whereas the Na contents remain very low.

Sodalite foyaite. In general, apatite is very scarce in the sodalite foyaite and was not observed by either Ussing (1912) or Ferguson (1964). However, in the sample examined in this study, apatite is abundant and occurs mainly as inclusions in the hedenbergite cores and their aegirine-hedenbergite rims.

A comparison with apatite from the less-evolved rocks in the roof sequence (pulaskite and foyaite) makes it possible to identify three apatite generations in the sodalite foyaite sample (Rønsbo, 1986; Rønsbo, unpublished data): (1) primary apatite belonging to the anhydrous high-temperature liquidus mineral assemblage, (2) irregularly zoned apatite representing altered primary apatite, and (3) late apatite occurring as euhedral crystals intergrown with arfvedsonite and nepheline and as overgrowths on second-generation apatite. The late apatite was formed during the late magmatic stage as defined by Larsen (1977). The present study only deals with the first and third types of apatite, which crystallized from liquids with quite different peralkalinity.

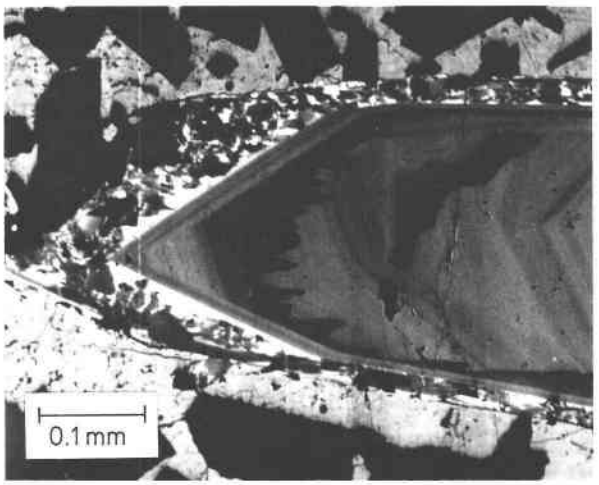

Fig. 3. Backscattered-electron image of apatite in quartz-bearing peralkaline pegmatite showing oscillatory-zoned core and irregularly zoned rim.

The primary apatite in the sodalite foyaite has oscillatory zoning with a zone width varying from 0.1 to approximately 20 μm. Selected microprobe analyses (4 and 5) showing minimum and maximum REE content are given in Table 4. These two analyses resemble the REE-rich apatite analyses from the augite syenite in all respects, except for a slight increase in the Na content.

Selected electron-microprobe analyses (1–4) of the late apatite are given in Table 5. These apatites are characterized by (1) distinct enrichment in Si and Na with increasing REE content and (2) a very pronounced relative heavy-REE depletion compared to the primary apatite.

Peralkaline pegmatite. Apatite is abundant in the peralkaline pegmatite. It occurs as prismatic crystals ranging from a few tenths of a millimeter up to almost 1 cm. All of the euhedral crystals examined with a length greater than 0.3 cm have oscillatory-zoned cores and irregularly zoned margins (Fig. 3), whereas most smaller crystals are irregularly zoned. Selected microprobe analyses (5–7) showing the compositional variation are given in Table 5. Like the late apatite in the sodalite foyaite, these apatites have a much higher La than Nd content. The most striking feature, however, is the increasing REE content accompanied by a pronounced Na enrichment and a low (0.17 to 0.39 wt%) SiO_2 content. A slightly higher SiO_2 content is observed in the irregularly zoned part of the crystals.

DISCUSSION AND INTERPRETATION

Coupled substitutions

Inspection of analytical data in Tables 4 and 5 reveals that the necessary charge balancing during the REE^{3+}

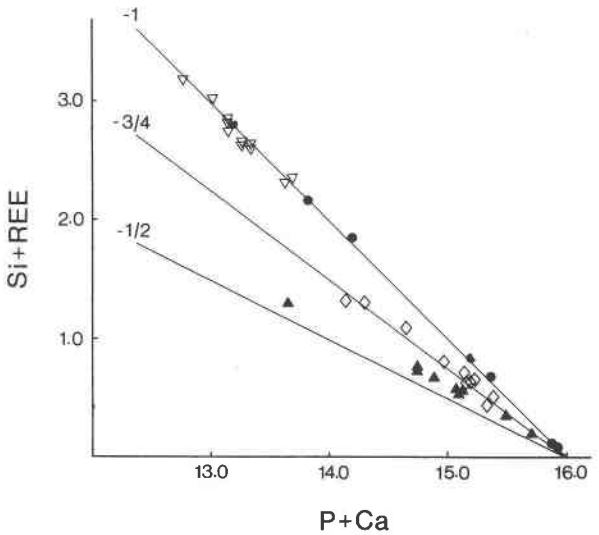

Fig. 4. Diagram showing variation of (P + Ca) versus (Si + REE) in apatite. Symbols: ● augite syenite, ▽ sodalite foyaite (Na-poor apatite), ◇ sodalite foyaite (Na-rich apatite), ▲ quartz-bearing peralkaline pegmatite. The three lines through the point (16,0) have the slopes −1, −¾ and −½. The line with the slope −1 represents the coupled substitution $REE^{3+} + Si^{4+} \rightleftharpoons Ca^{2+} + P^{5+}$.

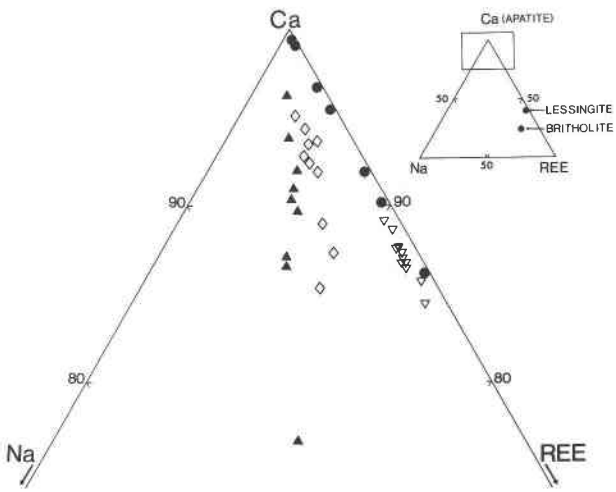

Fig. 5. Diagram showing Ca-REEs-Na content of apatites. Symbols: ● augite syenite, ▽ sodalite foyaite (Na-poor apatite), ◇ sodalite foyaite (Na-rich apatite), ▲ quartz-bearing peralkaline pegmatite.

substitution for Ca^{2+} in the apatite structure involves Si^{4+} and Na^{+}.

An experimental investigation by Ito (1968) substantiates the existence of complete solid solution between apatite ($Ca_5(PO_4)_3OH$) and lessingite-(Y) ($Y_3Ca_2(SiO_4)_3OH$) under experimental hydrothermal conditions (500–700 °C, 2 kbar), but only incomplete solid solution between apatite and lessingite-(La) ($Ca_2La_3(SiO_4)_3OH$). In both series, the coupled substitution follows the scheme: $Ca^{2+} + P^{5+} \rightleftharpoons REE^{3+} + Si^{4+}$. This REE enrichment in apatite can be best illustrated in a (Ca + P) versus (Si + REE) diagram, where the compositions will plot on a line, passing through the point (16,0), and with a slope of −1 (Fig. 4). The diagram clearly shows that apatites from the augite syenite and the primary apatite in sodalite foyaite plot along this line, which represents enrichment of the "lessingite" end-member in apatite. The analyses of the Na-enriched, late apatite in the sodalite foyaite scatter around a line with a slope of −¾, and the apatites from the peralkaline pegmatite approach a line with a slope of −½.

A plot of the analytical data on a Ca-REE-Na triangle (Fig. 5) reveals that apatite from the peralkaline pegmatite closely follows a trend defined by the substitution $2Ca^{2+} \rightleftharpoons Na^{+} + REE^{3+}$. These analyses fall close to the line passing through the point (16,0) with a slope of −0.5 (Fig. 4). The presence of the $2Ca^{2+} \rightleftharpoons Na^{+} + REE^{3+}$ substitution in apatite has been suggested by Rønsbo (1986) and Roeder et al. (1987). The late apatite from the sodalite foyaite represents an intermediate compositional trend, the result of almost equal contributions from the two coupled substitutions.

Na- and REE-enriched apatite analogues are known as the mineral britholite $(Na,Ca,REE)_5(SiO_4,PO_4)_3(OH,F)$, and various Na-REE silicophosphates and silicates have been synthesized by Ito (1968). Neither britholite nor the synthetic phases, however, resemble the theoretical end-member $Na_5REE_5(PO_4)_6(OH,F)_2$ for this part of a new solid-solution series. The partial apatite data given by Larsen (1979) as well as the composition of apatite from Pajarito (Roeder et al., 1987) represent extensive substitution toward this end-member.

Petrological implications

The coupled substitutions $Ca^{2+} + P^{5+} \rightleftharpoons REE^{3+} + Si^{4+}$ and $2Ca^{2+} \rightleftharpoons Na^{+} + REE^{3+}$ indicate that both the alkalinity and the silica activity of the liquid from which apatite crystallizes may control the composition of the REE-enriched apatite (Roeder et al., 1987). Experimental investigation of apatite crystallization and dissolution in crustal melts (Watson and Green, 1981) showed that the REE content of apatite is dependent on both the silica activity and the temperature of the magma. The apatite/liquid REE partition coefficients increase with increasing silica activity and with decreasing temperature. However, there are no experimental data on the stability and compositional variation of REE-enriched apatite with respect to magma alkalinity.

The four generations of apatites from the augite syenite and sodalite foyaite examined in this study have crystallized from magmas ranging in composition from syenite to agpaitic nepheline syenite. For this reason, the results presented here give some indication of the relationship between changes in magma composition and the compositional variation of REE-enriched apatite. The present

data show that in the nonperalkaline and slightly peralkaline environment (augite syenite and the early magmatic stage of the roof sequence, respectively), the substitution $REE^{3+} + Si^{4+} \rightleftharpoons Ca^{2+} + P^{5+}$ predominates and the $2Ca^{2+} \rightleftharpoons Na^{+} + REE^{3+}$ substitution appears to be unimportant. However, this latter substitution is found in apatite from the highly peralkaline environment (late magmatic stage of the roof sequence).

It is worth noting that late-formed apatites from the augite syenite and the sodalite foyaite display an increase in La:Nd ratios compared to the early-formed apatites. Also the total REE content and the La:Nd ratios for the late-formed apatite in the augite syenite are very similar to the primary apatite in the sodalite foyaite. Consequently, information on the evolution of highly evolved intrusions and their related dikes can be obtained from apatite by determination of the REE content, the form of the chondrite-normalized pattern, and the ratio between the two types of substitutions.

Acknowledgments

Thanks are due to L. M. Larsen and H. Bohse for provision of study samples. Suggestions and criticisms of my colleagues J. C. Bailey, L. M. Larsen, and A. K. Pedersen and the associate editor F. F. Foit, Jr., are gratefully acknowledged. The electron-microprobe facility is financed by the Danish Natural Science Research Council. This paper was authorized by the Director of the Geological Survey of Greenland.

References cited

Andersen, S., Bohse, H., and Steenfelt, A. (1981) A geological section through the southern part of the Ilímaussaq intrusion. Rapport Grønlands geologiske Undersøgelse, 103, 39–42.

Bailey, J.C., Larsen, L.M., and Sørensen, H. (1981) Introduction to the Ilímaussaq intrusion with a summary of the reported investigations. Rapport Grønlands geologiske Undersøgelse, 103, 5–17.

Blaxland, A.B., van Breeman, O., and Steenfelt, A. (1976) Age and origin of agpaitic magmatism at Ilímaussaq, South Greenland: Rb-Sr study. Lithos, 9, 31–38.

Drake, M.J., and Weill, D.F. (1972) New rare earth element standards for electron microprobe analysis. Chemical Geology, 10, 179–181.

Emeleus, C.H., and Upton, B.G.J. (1976) The Gardar period in southern Greenland. In A. Escher and W.S. Watt, Eds., Geology of Greenland, p. 152–181. Geological Survey of Greenland, Copenhagen.

Ferguson, J. (1964) Geology of the Ilímaussaq intrusion, South Greenland. Part I. Description of map and structure. Bulletin Grønlands geologiske Undersøgelse, 39, 81 p.

Ito, J. (1968) Silicate apatites and oxyapatites. American Mineralogist, 53, 890–907.

Larsen, L.M. (1976) Clinopyroxenes and coexisting mafic minerals from the alkaline Ilímaussaq intrusion, South Greenland. Journal of Petrology, 17, 258–290.

——— (1977) Aenigmatites from the Ilímaussaq intrusion, south Greenland: Chemistry and petrological implications. Lithos, 10, 257–270.

——— (1979) Distribution of REE and other trace elements between phenocrysts and peralkaline undersaturated magmas, exemplified by rocks from the Gardar igneous province, South Greenland. Lithos, 12, 303–315.

Larsen, L.M., and Sørensen, H. (1987) The Ilímaussaq intrusion—Progressive crystallization and formation of layering in an agpaitic magma. In J.G. Fitton and B.G.J. Upton, Eds., Alkaline igneous rocks. Geological Society of London Special Publication 30, p. 473–488.

Roeder, P.L. (1985) Electron-microprobe analysis of minerals for rare-earth elements: Use of calculated peak-overlap corrections. Canadian Mineralogist, 23, 263–271.

Roeder, P.L., MacArthur, D., Ma, X.P., and Palmer, G.R. (1987) Cathodoluminescence and microprobe study of rare-earth elements in apatite. American Mineralogist, 72, 801–811.

Rogers, P.S.Z., Duffy, C.J., Benjamin, T.M., and Maggiore, C.J. (1984) Geochemical applications of nuclear microprobes. Nuclear Instruments and Methods in Physics Research, B3, 671–676.

Rønsbo, J.G. (1986) Rare earth element enrichment in apatite from peralkaline undersaturated rocks. International Mineralogical Association Abstracts with Program, 215.

Sørensen, H. (1978) The position of the augite syenite and pulaskite in the Ilímaussaq intrusion, South Greenland. Bulletin of the Geological Society of Denmark, 27, special issue, 15–23.

Steenfelt, A. (1981) Field relations in the roof zone of the Ilímaussaq intrusion with special reference to the position of the alkali acid rocks. Rapport Grønlands geologiske Undersøgelse, 103, 43–52.

Upton, B.G.J. (1974) The alkaline province of South-West Greenland. In H. Sørensen, Ed., The alkaline rocks, p. 221–238. Wiley, London.

Ussing, N.V. (1912) Geology of the country around Julianehaab, Greenland. Meddelelser om Grønland, 38, 376 p.

Watson, E.B., and Green, T.H. (1981) Apatite/liquid partition coefficients for the rare earth elements and strontium. Earth and Planetary Science Letters, 56, 405–421.

Young, E.J., Myers, A.T., Munson, E.L., and Conklin, N.M. (1969) Mineralogy and geochemistry of fluorapatite from Cerro de Mercado, Durango, Mexico. U.S. Geological Survey Professional Papaer 650-D, D84–D93.

Manuscript received September 20, 1988
Manuscript accepted March 7, 1989